Cell, Vol. 97, 917–926, June 25, 1999, Copyright ©1999 by Cell Press

Chimeric Axon Guidance Receptors: The Cytoplasmic Domains of Slit and Netrin Receptors Specify Attraction versus Repulsion

Greg J. Bashaw and Corey S. Goodman*
Howard Hughes Medical Institute
Department of Molecular and Cell Biology
University of California
Berkeley, California 94720

Summary

Frazzled (Fra) is the DCC-like Netrin receptor in *Drosophila* that mediates attraction; Roundabout (Robo) is a Slit receptor that mediates repulsion. Both ligands are expressed at the midline; both receptors have related structures and are often expressed by the same neurons. To determine if attraction versus repulsion is a modular function encoded in the cytoplasmic domain of these receptors, we created chimeras carrying the ectodomain of one receptor and the cytoplasmic domain of the other and tested their function in transgenic *Drosophila*. Fra-Robo (Fra's ectodomain and Robo's cytoplasmic domain) functions as a repulsive Netrin receptor; neurons expressing Fra-Robo avoid the Netrin-expressing midline and muscles. Robo-Fra (Robo's ectodomain and Fra's cytoplasmic domain) is an attractive Slit receptor; neurons and muscle precursors expressing Robo-Fra are attracted to the Slit-expressing midline.

Introduction

Growth cones are guided by both attractants and repellents, and these signals can be either short range or long range. Thus, there are four major guidance forces: contact–attraction, chemoattraction, contact–repulsion, and chemorepulsion (Tessier-Lavigne and Goodman, 1996). With the search for guidance molecules mediating these mechanisms came the expectation that distinct families of proteins might be found that fit these categories. But with the discoveries of novel families of guidance molecules came the unexpected result that many of these molecules are bifunctional, mediating either attraction or repulsion, depending on the context. Netrins, for example, can be both attractive and repulsive (Hedgecock et al., 1990; Serafini et al., 1994; Colamarino and Tessier-Lavigne, 1995; Winberg et al., 1998a). The same now appears to be true for Semaphorins (Kolodkin et al., 1993; Luo et al., 1993; Wong et al., 1997; Bagnard et al., 1998). Most recently, compelling data have revealed multiple functions for Slits (Brose et al., 1999; Kidd et al., 1999; Li et al., 1999; Wang et al., 1999). If the ligands are intrinsically indeterminate, then the key to the sign of the response is likely to reside in either some property of the receptor or receptor complex. Alternatively, differences in the internal state of the growth cone and/or differential expression of cytoplasmic signaling components could influence the sign of growth cone response.

*To whom correspondence should be addressed.

In the present study, we asked where attraction versus repulsion is encoded. Netrin and Slit receptors in *Drosophila melanogaster* provide an ideal opportunity to answer this question. In *Drosophila*, both Netrins (NetA and NetB) (Harris et al., 1996; Mitchell et al., 1996) and Slit (Rothberg et al., 1990; Kidd et al., 1999) are expressed by the same midline cells. At the *Drosophila* midline, Netrins function largely as attractants. This attractive function is mediated by Frazzled (Fra) (Kolodziej et al., 1996), a member of the Deleted in Colorectal Cancer (DCC)/UNC-40 family of Netrin receptors (Chan et al., 1996; Keino-Masu et al., 1996). Slit, on the other hand, functions as a midline repellent. This repulsive function is mediated largely by Roundabout (Robo) (Kidd et al., 1998a, 1999; Brose et al., 1999). Fra and Robo are related proteins; both are members of the immunoglobulin (Ig) superfamily. The ectodomain of Fra consists of four Ig domains followed by six fibronectin (FN) type III repeats: Fra has a cytoplasmic domain of 278 amino acids. Robo has an ectodomain of five Ig domains followed by three FN III repeats: Robo has a cytoplasmic domain of 457 amino acids. Neither cytoplasmic domain has any obvious catalytic signaling motif, but both have proline-rich regions and other short stretches of evolutionarily conserved sequences (Kolodziej et al., 1996; Kidd et al., 1998a).

Given that many growth cones near the midline simultaneously integrate attractive and repulsive signals from Fra and Robo, it seemed likely to us that the components that mediate attraction versus repulsion are ubiquitous and that the difference between attraction and repulsion is encoded in the sequence of these receptors. One model would predict that guidance receptors are modular, with ectodomains determining ligand binding and cytoplasmic domains specifying effector function. If this is correct, then swapping the cytoplasmic domains of Fra and Robo should generate chimeric receptors with the ligand binding property of one receptor and the effector function of another. If all growth cones have the necessary machinery to respond to these cytoplasmic signals, then we should be able to change growth cone behavior in vivo by transgenically driving the expression of these chimeric receptors.

To test this model, we exchanged the cytoplasmic domains of Fra and Robo and then generated transgenic fruit flies expressing these chimeric receptors on all or a subset of developing axons utilizing the GAL4–UAS two-component system (Brand and Perrimon, 1993). The model predicts that Fra-Robo should be a novel repulsive Netrin receptor and that Robo-Fra should be a novel attractive Slit receptor. In this paper, we show that both chimeric receptors behave just as predicted. Growth cones expressing Fra-Robo are repelled by Netrin-expressing midline cells, leading to a Netrin-dependent phenotype in which too few axons cross the midline. Growth cones expressing Robo-Fra are attracted to the Slit-expressing midline cells, leading to a phenotype in which too many axons cross and/or grow along the midline.

All growth cones appear capable of using these chimeric

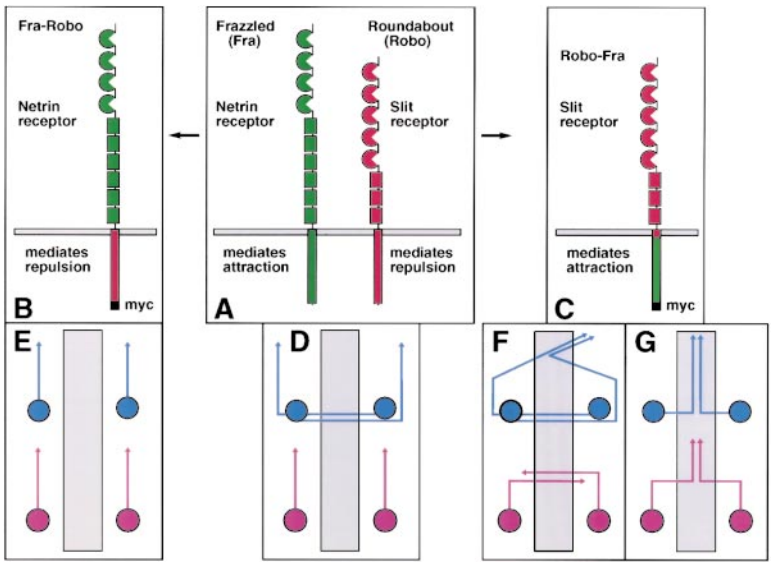

Figure 1. Summary of Chimeric Receptors and Transgenic Phenotypes

(A) The structure of the wild-type Frazzled and Robo receptors is indicated. Frazzled, shaded green, consists of an ectodomain that has four immunoglobulin (Ig) domains (broken circles), six fibronectin type III (FN III) repeats (rectangles), and a long cytoplasmic domain. It normally mediates attraction in response to Netrin at the midline. Robo, shaded red, has an ectodomain with five Ig domains, three FN III repeats, and a long cytoplasmic domain. It normally mediates repulsion in response to Slit at the midline.

(B) The Frazzled-Robo (Fra-Robo) chimera consists of the ectodomain of Fra fused to the transmembrane and cytoplasmic domains of Robo. The C-terminal six Myc tag used to monitor expression is indicated. The prediction is that this chimera should now mediate repulsion in response to Netrin.

(C) The Robo-Frazzled (Robo-Fra) chimera has the extracellular, transmembrane, and 67 amino acids of Robo's cytoplasmic domain (red) fused to the entire cytoplasmic domain of Fra (green). The C-terminal six Myc tag is indicated. This chimera should now mediate attraction in response to Slit.

(D) The behavior of two different classes of CNS interneurons is diagrammed. The midline, which normally expresses both Netrins and Slit, is represented by a gray box. Axons of commissural interneurons (colored blue) are attracted to Netrin expressed at the midline (e.g., SP1 as shown schematically here). They cross the midline and then project ipsilaterally along it. Once they have crossed the midline, upregulation of the Robo receptor prevents them from recrossing. Axons of longitudinal interneurons (colored purple) are repelled by Slit expressed at the midline (e.g., pCC as shown schematically here). They never cross the midline but instead project ipsilaterally along it.

(E) The phenotype resulting from pan-neural expression of Fra-Robo is shown. Instead of being attracted to Netrin at the midline, axons of the commissural interneurons (blue) are repelled. This phenotype is similar to a *commissureless* loss of function.

(F) The weaker phenotype resulting from pan-neural expression of Robo-Fra is shown. Instead of being repelled by Slit at the midline, longitudinal axons (purple) are attracted to Slit and freely cross and recross the midline. Commissural axons (blue) now freely cross and recross the midline as well. This phenotype is similar to a *robo* loss of function.

(G) The stronger phenotype resulting from pan-neural expression of Robo-Fra is shown. This phenotype is driven by increased expression. All axons enter and then grow along the midline. This phenotype is similar to a *slit* loss of function.

receptors. The chimeric receptors, when expressed at high levels, dominate the growth cone's response and appear to overshadow the function of the normal Netrin and Slit receptors. The strength of the phenotypes is highly dose dependent. Interestingly, migrating muscle precursors expressing Robo-Fra respond to Slit in the same fashion as do Robo-Fra-expressing growth cones. Thus, although these muscle precursors are normally repelled by the midline, they contain the necessary machinery to generate the attractive response mediated by Fra's cytoplasmic domain, even though they normally do not express Fra.

Results

Constructs and Phenotypic Predictions

We exchanged the cytoplasmic domains of the Fra attractive guidance receptor and the Robo repulsive guidance receptor (Figures 1A–1C). The two constructs were cloned downstream of UAS activation sequences to allow targeted misexpression using various GAL4 lines (Brand and Perrimon, 1993). Based on the midline expression patterns of Netrin (Harris et al., 1996; Mitchell et al., 1996) and Slit (Rothberg et al., 1990; Kidd et al., 1999), there are clear phenotypic predictions about the consequences of pan-neural overexpression of the two chimeras. In the case of Fra-Robo (Figure 1B), we predict that growth cones expressing this chimera would be repelled by Netrin secreted from the midline glia, leading to a phenotype in which too few axons cross the midline (Figure 1E). We make the opposite prediction for Robo-Fra (Figure 1C): growth cones expressing Robo-Fra should now be attracted to the Slit protein, and too many axons should cross and/or grow along the midline (Figures 1F and 1G). As described below, our results confirm both predictions.

Pan-Neural Expression of Fra-Robo Directs Axons Away from Netrin

Flies carrying *fra-robo* transgenes and flies carrying *elav-GAL4* were crossed together to generate animals that express Fra-Robo in all neurons during development, beginning at the time of axon outgrowth. Embryos carrying one copy of the *fra-robo* transgene and one copy of the *elav-GAL4* driver have commissures that are significantly thinner than wild type (Figures 2A and 2B). These animals are viable and when crossed to each other generate embryos expressing higher levels of Fra-Robo. The progeny of these crosses show phenotypes ranging from wild type to completely commissureless (Figure 2C). The severity of the CNS phenotype strongly correlates with the level of Fra-Robo expression. This commissureless phenotype is consistent with the idea that the Fra-Robo receptor is interpreting Netrin as a repulsive cue and that the cytoplasmic domain of Robo can generate a repulsive response independent of the specific identity of the extracellular ligand.

In addition to guiding a subset of commissural axons

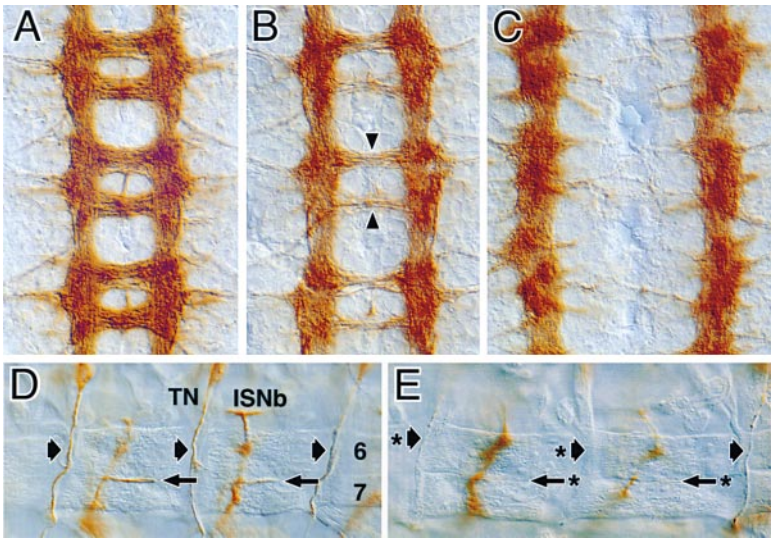

Figure 2. Neurons Expressing Fra-Robo Are Repelled by Cells Expressing Netrin

(A) A stage 16 wild-type embryo stained with the monoclonal antibody (mAb) BP102 to reveal the CNS axon scaffold. Anterior is up.

(B) A stage 16 embryo carrying one copy of *elav-GAL4* and one copy of the *fra-robo* transgene stained with BP102. Both the anterior and posterior commissures are significantly thinner (arrowheads).

(C) A stage 16 embryo carrying two copies of *elav-GAL4* and two copies of the *fra-robo* transgene stained with BP102. Commissures are completely absent.

(D) Two hemisegments from a stage 17 wild-type embryo stained with a monoclonal antibody against Fasciclin II (1D4) to reveal the major motor projections in the region of the ventral longitudinal muscles. The focal plane is the cleft between muscles 7 and 6. Broad arrows indicate the position of the transverse nerves (TN) that form just over muscles 7 and 6. Arrows indicate normal innervation of muscles 7 and 6 by the RP3 motoneuron in the ISNb motor nerve. Anterior is left and dorsal is up.

(E) Two hemisegments from a stage 17 embryo expressing high levels of Fra-Robo stained with 1D4. The RP3 motoneuron has failed to innervate muscles 7 and 6 in both segments (arrows with asterisks). Two of the three TNs have stalled and have failed to cross muscles 7 and 6 (broad arrows with asterisks). Anterior is left and dorsal is up.

across the midline, Netrin also guides certain motor axons to their correct muscle targets (Mitchell et al., 1996; Winberg et al., 1998a). NetB (one of the two *Drosophila* Netrins) is expressed by ventral muscles 7 and 6, where it provides an attractive cue to growth cones of the RP3 motoneuron. We examined the motor projections in embryos expressing high levels of Fra-Robo with a monoclonal antibody against Fasciclin II (Fas II; 1D4) (Van Vactor et al., 1993) to determine if there are defects in innervation of muscles 7 and 6 and/or other motor axon guidance defects consistent with Netrin acting as a repulsive cue. We observe a dramatic reduction in innervation at muscles 7 and 6 (78%, n = 155), as well as other defects in the intersegmental nerve b (ISNb) pathway (predominantly bypass and stalls) as compared to wild type, suggesting that the normal Netrin expression by these two muscles is repelling the Fra-Robo-expressing motor growth cones (Figures 2D and 2E). In contrast to *fra* and *Netrin* mutants, in which the ISN frequently crosses the segment border and fasciculates with the ISN in the adjacent segment, we do not observe this phenotype in *fra-robo* gain-of-function animals.

We also see defects in the projection of the transverse nerve (TN). In wild-type embryos, a peripheral neuron, the LBD cell, projects one axon distally toward the alary muscle and another axon proximally toward the CNS. Early in stage 16, the proximally projecting LBD axon meets and fasciculates with one of the distally projecting TMN axons to form the TN (Figure 2D). This occurs near the segment border just adjacent to muscle 7 (see Winberg et al. [1998a] for details and references). The projection of the TN is not affected in *Netrin* or *fra* mutants. However, in embryos expressing high levels of Fra-Robo, the TN fails to form over muscles 7 and 6, suggesting that these axons are also now repelled by the Netrin expressed by muscles 7 and 6 (Figure 2E); both branches (the LBD and the TMN axons) stall and do not enter the region of the ventral muscles (75%, n = 148). This phenotype is very similar to what is seen when the chemorepellent Semaphorin II (Sema II) is ectopically expressed by these muscles (Winberg et al., 1998a).

It is important to distinguish between true gain-of-function phenotypes of the chimera and the potential dominant-negative effects of overexpressing the Fra extracellular domain. The dramatic difference between the Fra-Robo expression phenotypes and the *fra* loss-of-function phenotypes argues against the dominant-negative hypothesis. If Fra-Robo were a dominant negative for *fra* function, we would expect its phenotype to mimic *fra* loss of function. However, *fra-robo* phenotypes are stronger and qualitatively different than *fra* loss-of-function phenotypes, both in the CNS and the periphery. Furthermore, overexpression of a truncated Fra receptor (see Experimental Procedures) does not generate dominant phenotypes (data not shown). Taken together, these observations suggest that Fra-Robo is not a Fra dominant negative but rather that it senses Netrin as a repulsive cue.

The Fra-Robo Expression Phenotype Is Dependent on Netrin but Not on Frazzled

Since the *fra-robo* gain-of-function phenotype is considerably stronger than either the *Netrin* or *fra* loss-of-function phenotypes, we wanted to determine whether either of these two mutations would be epistatic to *fra-robo*. A strong prediction of the model that the Fra-Robo receptor is interpreting Netrin as a repulsive cue is that the commissureless phenotype should be dependent on *Netrin* but not on *fra* function. Therefore, we examined the effects of removing *Netrin* or *fra* function from *fra-robo* gain-of-function embryos.

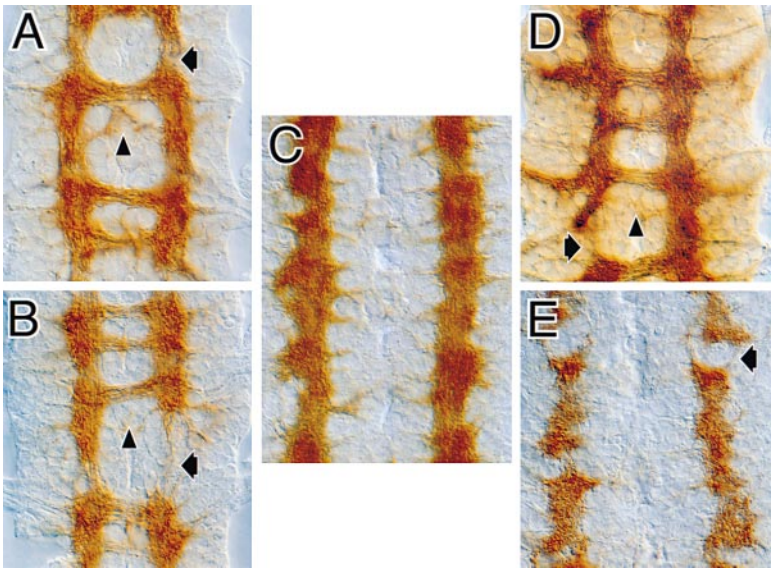

Figure 3. Epistasis Analysis of the *fra-robo* Gain-of-Function Phenotype

All embryos pictured are stage 16 and have been stained with mAb BP102 and filleted to reveal the CNS axon scaffold. Anterior is up.

(A) A *Netrin* NP5 deficiency (removing both tandem *Netrin* genes) embryo shows a characteristic *Netrin* loss-of-function phenotype. The central segment is missing the posterior commissure (arrowhead), and there are breaks in the longitudinal connectives (broad arrow).

(B) A *fra* null mutant embryo is phenotypically similar to the *Netrin* deficiency embryo. Commissures are thin or absent (arrowhead), and there are breaks in the longitudinal connectives (broad arrow).

(C) The characteristic commissureless phenotype of an embryo expressing high levels of the Fra-Robo chimera is shown.

(D) A *Netrin* NP5 deficiency embryo that is also expressing high levels of the Fra-Robo chimera. In this case, the embryo was also stained with the monoclonal anti-Myc antibody to reveal the presence of Fra-Robo expression. The Myc staining can be seen as a light brown cast over the nerve cord. Note the characteristic *Netrin* loss-of-function phenotype with thin or absent posterior commmisures (arrowhead) and breaks in the longitudinal connectives (broad arrow). Thus, the *Netrin* deficiency suppresses the *fra-robo* gain of function phenotype.

(E) A *fra* null mutant embryo that is also expressing high levels of the Fra-Robo chimera. This animal is still completely commissureless, indicating that loss of *fra* function does not suppress the *fra-robo* gain-of-function phenotype. However, the phenotypes appear to be additive in that we observe effects of the *fra* mutation on the integrity of the longitudinal axon tracts (broad arrow).

Netrin and *fra* mutants display similar CNS loss-of-function phenotypes in which too few axons cross the midline and there are occasional breaks and general disorganization in the longitudinal tracts (Figures 3A and 3B) (Harris et al., 1996; Kolodziej et al., 1996; Mitchell et al., 1996). Both mutations affect the posterior commissure more strongly than the anterior (Figures 3A and 3B). In contrast, Fra-Robo expression gives a completely commissureless phenotype (Figure 3C). Removing *Netrin* function with a deficiency that takes out both *Netrin* genes (Winberg et al., 1998a) in combination with *fra-robo* results in a *Netrin* phenotype (Figure 3D), allowing significant formation of many commissures (see Experimental Procedures for details). In contrast, removing *fra* function has no effect on the *fra-robo* commissureless phenotype; rather, the two phenotypes appear to be additive: commissures do not form, but breaks are observed in the longitudinal connectives (Figure 3E). Together with the phenotypic evidence, these genetic observations further argue that the Fra-Robo chimera responds to Netrin as a repulsive cue.

Overexpression of Comm Suppresses the *fra-robo* Gain-of-Function Phenotype

In contrast to the endogenous Fra receptor, which is expressed uniformly on all CNS axons (Kolodziej et al., 1996), the endogenous Robo receptor exhibits a striking localization pattern. It is expressed at high levels on longitudinal axons but is greatly reduced or absent on commissural axons (Kidd et al., 1998a). This localization appears to reflect posttranslational regulation, because the same restricted expression pattern is observed when a Robo cDNA lacking untranslated regions is overexpressed in all neurons (Figure 4A) (Kidd et al., 1998a). The presence of Robo protein in the commissures of flies carrying hypomorphic mutations in the *commissureless(comm)* gene indicates a role for *comm* in preventing Robo accumulation in the commissures. Genetic and transgenic analyses have revealed that a critical function of the Comm protein is to downregulate Robo protein levels on axons that cross the midline (Kidd et al., 1998b). It is not known what part of the Robo protein responds to Comm regulation, nor is it known what part of the Robo protein confers restriction to the longitudinal axon tracts.

To determine whether this regulatory information is present in the cytoplasmic domain (or transmembrane domain) of the Robo receptor, we examined the localization of the Fra-Robo receptor using the C-terminal Myc epitope tag. We chose a weakly expressed insert of the *fra-robo* transgene because embryos carrying this insert do not display any mutant phenotype (data not shown). Like the endogenous Robo receptor, the Fra-Robo receptor is restricted to the longitudinal axon tracts (Figure 4B). This suggests that the cytoplasmic domain (or transmembrane domain) of Robo can confer longitudinal localization.

The longitudinal localization of Fra-Robo suggested that Fra-Robo might be regulated by Comm. To test this hypothesis, we simultaneously expressed Comm and Fra-Robo in all neurons. We find that the *fra-robo* gain-of-function phenotype is significantly suppressed (Figures 4C and 4D; see Experimental Procedures). Furthermore, anti-Myc staining reveals that in embryos overexpressing both *fra-robo* and *comm*, the axonal expression of Fra-Robo is greatly reduced (data not shown). This argues that the cytoplasmic domain (or transmembrane domain) of Robo is the target for the Comm-mediated downregulation of Robo function.

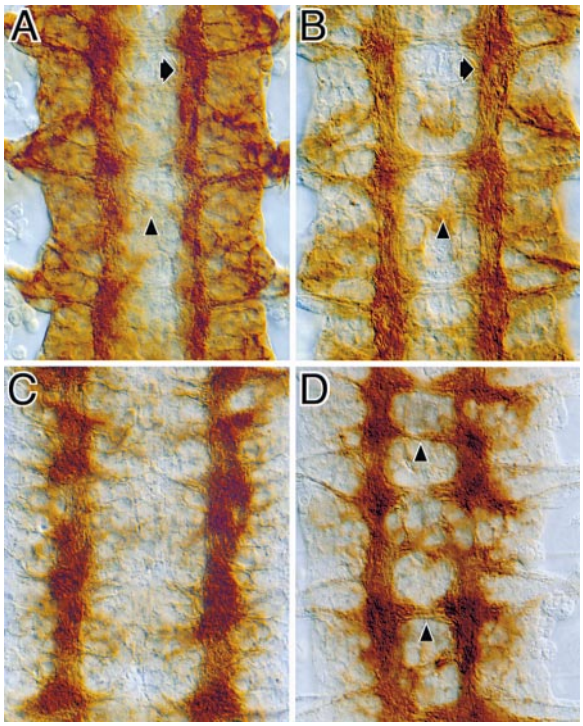

Figure 4. Regulation of Fra-Robo

(A) A stage 16 embryo carrying one copy of *UAS-robo* and one copy of *elav-GAL4* stained with the anti-Robo mAb. As reported previously by Kidd et al. (1998a), Robo expression is seen at high levels on the longitudinal axon tracts (broad arrow), while very little Robo expression is detected in the commissures (arrowhead).

(B) A stage 16 embryo carrying one copy of a weak insert of the *fra-robo* transgene and one copy of *elav-GAL4* stained with the anti-Myc mAb to reveal the expression of the Fra-Robo chimera. Fra-Robo expression is observed at high levels in the longitudinal axons (broad arrow) but at very low levels in the commissures (arrowhead). This expression is nearly identical to that seen by native Robo.

(C) A stage 16 embryo expressing high levels of the Fra-Robo chimera stained with BP102 is shown. Note the characteristic commissureless phenotype.

(D) In addition to carrying an equivalent dose of the *fra-robo* transgene as the embryo shown in (C), this BP102-stained stage 16 embryo also carries one copy of a *UAS commissureless* transgene. This embryo shows significant rescue of the commissures (arrowheads), indicating a partial suppression of the *fra-robo* gain-of-function phenotype. This suggests that Comm is likely to be downregulating Fra-Robo just as it does Robo.

Robo-Fra Expression Results in Guidance Defects Complementary to Fra-Robo

Consistent with the prediction that axons expressing the Robo-Fra chimera would now be attracted to Slit protein at the midline, we find that embryos carrying a single copy of a *robo-fra* transgene and a single copy of *elav-GAL4* exhibit marked perturbation of the wild-type axon scaffold, with far too many axons crossing the midline (Figures 5A and 5D). These single-dose *robo-fra* embryos show a phenotype very similar to *robo* loss-of-function mutants (Figure 5B).

While the single-dose *robo-fra* phenotype fits the prediction that growth cones expressing this chimera are interpreting Slit as an attractive signal, it is also consistent with the idea that Robo-Fra is functioning as a Robo dominant negative. We therefore sought to express higher levels of Robo-Fra, reasoning that a dominant-negative Robo receptor should not be able to generate a phenotype that is stronger than *robo* loss of function, while a receptor that was sensing Slit as an attractive cue should have no such constraint and might generate a gain-of-function phenotype that approaches the stronger *slit* loss of function. By creating animals with different doses of the *robo-fra* transgene, we were able to generate a range of different expression levels and a corresponding phenotypic series (Figures 5D–5F). At intermediate levels of expression, Robo-Fra generates a CNS phenotype slightly stronger than *robo* null mutants (compare Figures 5B and 5E). At even higher levels, the CNS phenotype is markedly more severe than *robo* mutants and approaches the midline collapse phenotype characteristic of *slit* mutants (Figures 5C and 5F). These observations argue that Robo-Fra is responding to midline Slit protein as an attractive cue and that the cytoplasmic domain of Fra is able to access the machinery downstream of attractive guidance independent of Netrin.

Robo-Fra Does Not Act as a Dominant Negative

Although the severity of the high-level expression phenotype of *robo-fra* would seem to preclude the possibility that it is acting simply as a *robo* dominant negative, we cannot completely exclude the possibility that it is acting negatively. The difference between the *robo* receptor loss-of-function phenotype and the *slit* ligand loss-of-function phenotype suggests that there is at least one other Slit receptor in *Drosophila*. Indeed, there is another Robo-related protein, Robo2, that is a very good candidate to be a second Slit receptor (J. Simpson, T. Kidd, and C. S. G., unpublished). It is possible that rather than being attracted to Slit, the Robo-Fra receptor is a powerful dominant negative that blocks the function of both Robo receptors. In the case of the *fra-robo* chimera, the differences between the chimeric gain-of-function phenotype and the *fra* and *netrin* loss-of-function phenotypes allowed us to use epistasis analysis to confirm that the *fra-robo* gain of function is dependent on Netrin function and is not a Fra dominant negative. In the case of *robo-fra*, the similarity between the *robo-fra* gain-of-function phenotypes and the *slit* and *robo* loss-of-function phenotypes prohibits a similar genetic analysis. Therefore, in order to address the possibility that Robo-Fra acts as a dominant negative, we generated a Myc-tagged truncated Robo construct that has exactly the same Robo sequences as Robo-Fra but none of the Fra sequences (see Experimental Procedures). We directly compared the expression phenotypes of *robo-fra* with those of the truncated Robo construct *robo*Δ*C*. We used the Fas II monoclonal antibody (mAb; 1D4) because it stains a subset of axons that normally do not cross the midline (Figure 6A) and therefore provides a sensitive measure of whether axons are inappropriately crossing the midline. In addition to comparing the effect of pan-neural expression (*elav-GAL4*) of these constructs, we also compared the effects of expressing the two constructs with the *fushi tarazu neurogenic* element driving *GAL4(ftz$_{ng}$-GAL4)*, which drives expression in a subset of neurons whose axons do not normally cross the midline.

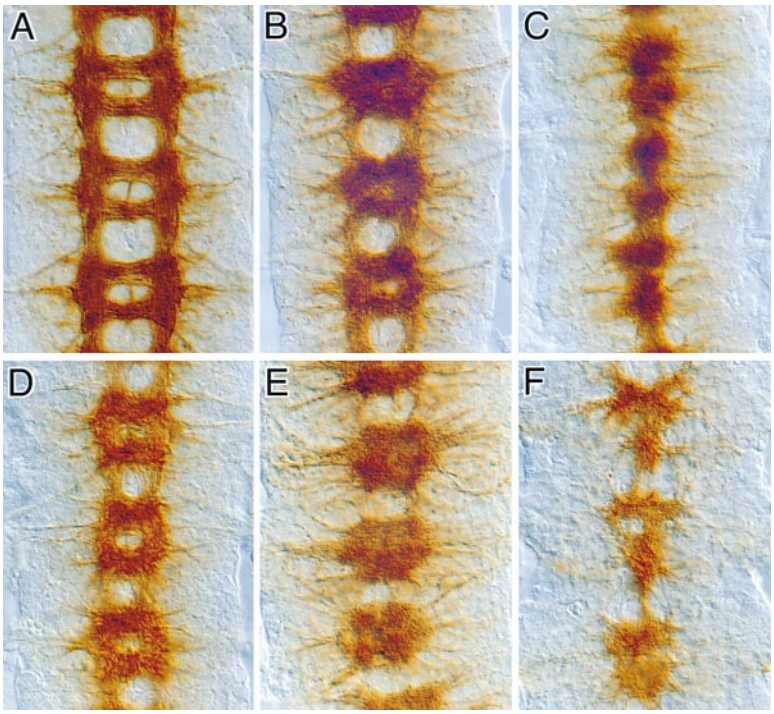

Figure 5. Neurons Expressing Robo-Fra Are Attracted by Cells Expressing Slit

All embryos pictured are stage 16 and have been stained with mAb BP102 and filleted to reveal the CNS axon scaffold. Anterior is up.
(A) A wild-type embryo.
(B) A *robo* null mutant embryo. Far too many axons cross and recross the midline, resulting in commissures that are much thicker than wild type and thinner longitudinal connectives.
(C) A *slit* null mutant embryo showing the characteristic collapse of all axons onto the CNS midline.
(D) An embryo carrying one copy of the *robo-fra* transgene and one copy of *elav-GAL4*. Like in the *robo* mutant, too many axons cross the midline, resulting in thick fuzzy commissures and thin longitudinal tracts.
(E) An embryo carrying two copies of the *robo-fra* transgene and one copy of *elav-GAL4*. The resulting phenotype is more severe than the single-copy animal in (D) and stronger than the *robo* mutant. Note the complete absence of space between the anterior and posterior commissures and the near absence of longitudinal tracts.
(F) An embryo carrying two copies of the *robo-fra* transgene and two copies of *elav-GAL4*. At these higher levels of Robo-Fra expression, the CNS axons now appear to have partially collapsed onto the midline. This phenotype is much stronger than that seen in the *robo* mutant and is approaching that seen in the *slit* mutant.

None of the four inserts of *robo*Δ*C* exhibit any CNS phenotype when expressed in single copy with *elav-GAL4*, while in the case of *robo-fra*, all of the inserts give strong CNS phenotypes in single copy. In addition, anti-Myc antibody staining reveals that the *robo-fra* and *robo*Δ*C* transgenes are expressed at comparable levels and show similar degrees of axonal expression (data not shown). At higher levels of expression, dominant-negative effects of *robo*Δ*C* are revealed and a *robo*-like phenotype results (Figure 6B). These phenotypes are not nearly as severe as those observed for *robo-fra* (Figure 6C) and never exceed the *robo* loss-of-function phenotype. Indeed, all of the *robo-fra* transgenes give comparable or stronger phenotypes in single copy than the strongest *robo*Δ*C* transgene when expressed in double copy (data not shown). Finally, we compared the effects of expressing the chimera and the dominant negative with ftz_{ng}*-GAL4*. We find that the highest dose of *robo*Δ*C* transgene in ftz^{+} neurons results in only very few axons inappropriately crossing the midline (Figure 6D), while ftz^{+} neurons expressing Robo-Fra readily cross or grow along the midline even at relatively low transgene dosages (Figure 6E and data not shown). The difference between the effects of *robo*Δ*C* in the two different cases examined could reflect a difference in the susceptibility of the ftz^{+} neurons to effects of the dominant negative. Perhaps since ftz^{+} neurons require Robo to prevent them from extending axons across the midline, they may represent a subset of neurons that normally expresses relatively higher levels of Robo and thus may be more resistant to the dominant negative. No such differential sensitivity between effects of ftz_{ng}*-GAL4* and *elav-GAL4* was observed for Robo-Fra. Taken together, these observations strengthen the conclusion that the Robo-Fra receptor does not act negatively, but rather that it acts as a true gain of function, responding to Slit as an attractive signal.

Mesodermal Expression of Robo-Fra Causes Muscles to Invade the Midline

In addition to functioning as a short-range repellent for axons navigating near the midline, Slit also functions as a long-range chemorepellent for migrating muscle precursors (Kidd et al., 1999). In wild-type *Drosophila* embryos, myoblasts initially migrate laterally away from the midline over the inside surface of the developing CNS. Later in development, some muscles extend back toward the ventral midline beneath (i.e., outside of) the developing CNS, attaching to the epidermis at a distance from the midline (Lewis and Crews, 1994). To determine whether expressing the Robo-Fra chimera on muscle precursors would affect their migration, we used the pan-mesodermal GAL4 line *24B-GAL4* to drive Robo-Fra expression. In contrast to wild-type embryos (Figure 7A), in embryos overexpressing Robo-Fra on all muscles, muscle precursors are observed extending toward and across the midline (Figures 7C and 7D). In addition to showing abnormal migration, the muscle precursors invading the midline also have unusual morphology, sending out many long thin filopodial and flattened lamellipodial extensions toward the Slit-expressing midline, suggesting that they are now attracted to

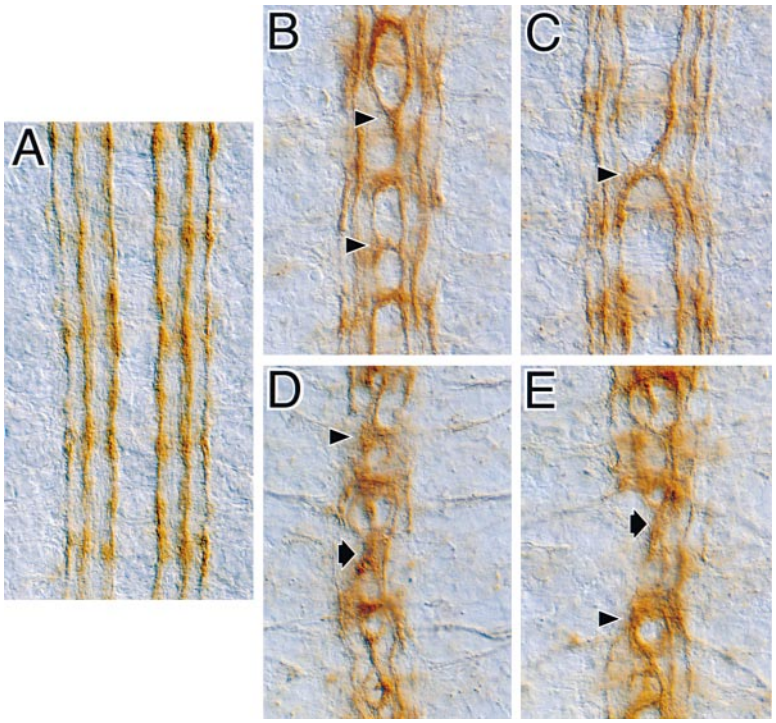

Figure 6. Robo-Fra Generates a Gain-of-Function Phenotype that Is Quantitatively and Qualitatively Different from the Robo Dominant Negative

Stage 15–16 embryos were stained with a mAb to Fas II (1D4). Anterior is up.

(A) A wild-type embryo stained with mAb 1D4. Fas II expression is observed in a subset of longitudinal axons that never cross the midline.

(B) An embryo carrying two copies of the *robo*Δ*C* transgene and two copies of *elav-GAL4*. Axons of the medial-most longitudinal pathway can be seen inappropriately crossing the midline (arrowheads). This phenotype is similar to the phenotype of *robo* loss-of-function mutants.

(C) An embryo carrying two copies of the *robo*Δ*C* transgene and two copies of ftz_{ng}-*GAL4*. In one segment, a bundle of axons of the medial-most pathway has inappropriately crossed the midline (arrowhead). This phenotype is much milder than that seen in the embryo in (B).

(D) An embryo carrying two copies of *robo-fra* and two copies of *elav-GAL4*. Axons from all three longitudinal pathways show abnormal trajectories. The severity of the phenotype shows some segmental variability. Some segments show a milder phenotype characteristic of *robo* mutants (arrowhead), while others show a more *slit*-like phenotype where several longitudinal pathways have collapsed in and are growing along the midline (broad arrow).

(E) An embryo carrying two copies of *robo-fra* and two copies of ftz_{ng}-*GAL4*. As in (D), some segments show a milder *robo*-like phenotype (arrowhead), while others are more compressed with multiple pathways growing along the midline (broad arrow). A comparison of the *robo*Δ*C* phenotypes in (B) and (C) with those of *robo-fra* in (D) and (E) shows that *robo-fra* phenotypes are much more severe, affecting multiple longitudinal pathways, than those of *robo*Δ*C*.

Slit (Figures 7C and 7D). Muscles at a distance from the midline, such as muscles 7 and 6, develop quite normally. The fact that only those muscles that are navigating near midline sources of Slit show these abnormal phenotypes and that expressing a normal Robo receptor or *robo*Δ*C* does not produce this effect argues that this phenomenon is specific to the chimera (Figure 7B and data not shown). These results support the conclusion that the Robo-Fra chimera can respond to Slit as both a long- and short-range attractant. Furthermore, these observations suggest that migrating muscle precursors use downstream signaling machinery similar to that of growth cones to respond to guidance cues in their environment.

Discussion

In this paper, we have shown that the cytoplasmic domain of a guidance receptor can determine the nature of the growth cone's response in vivo, independent of the ectodomain and its particular ligand binding. Fra (the DCC family receptor in *Drosophila*), which normally mediates an attractive response to Netrin, can instead mediate a repulsive response to Netrin when given the cytoplasmic domain from Robo. In contrast, Robo, which normally mediates a repulsive response to Slit, can instead mediate an attractive response to Slit when given the cytoplasmic domain of Fra. Thus, there is nothing intrinsically attractive or repulsive about a particular guidance signal, nor is there any information in the particular ligand-binding property of a receptor's ectodomain. Rather, and perhaps not surprisingly, the nature of the response is encoded in the cytoplasmic sequence. In short, these two guidance receptors are modular and their ectodomains and cytoplasmic domains are interchangeable.

In a companion paper (Hong et al., 1999 [this issue of *Cell*]), an independent in vitro study has come to a similar conclusion. Netrin receptors of the DCC family mediate attraction, while those of the UNC5 family mediate repulsion; in at least some cases, DCC proteins are required for UNC5 effects. A ligand-gated association between the cytoplasmic domains of UNC5 and DCC converts Netrin-mediated attraction to repulsion. A major conclusion of this study is that repulsion is encoded in the UNC5 cytoplasmic domain.

In *Drosophila*, the same midline cells normally secrete both Netrins and Slit. Growth cones can simultaneously respond to both ligands in a cell-specific fashion. Some growth cones express high levels of Fra and low levels of Robo, and they extend toward and across the midline. Other growth cones appear to express high levels of both receptors, and they can extend toward the midline, but they do not cross it (Kidd et al., 1998b). Growth cones can dramatically change their levels of Robo expression; once they cross the midline, growth cones increase their level of Robo, a change that prevents them from crossing the midline again (Kidd et al., 1998a, 1998b).

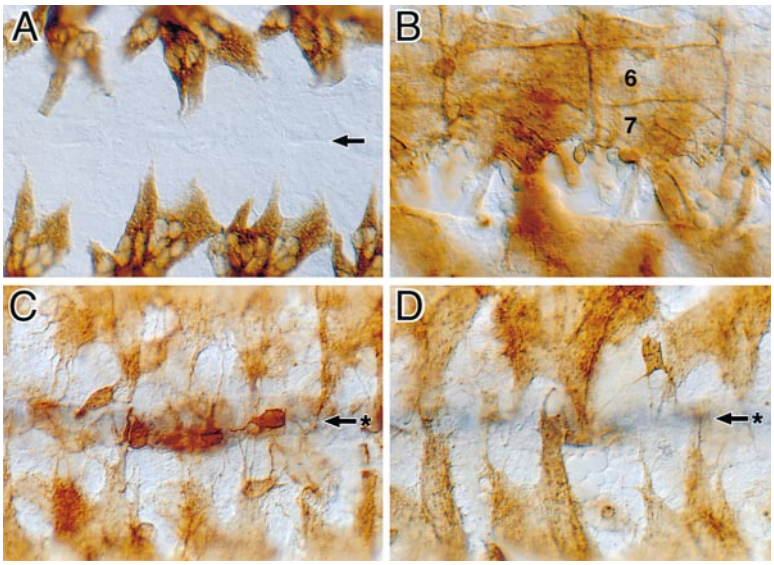

Figure 7. Robo-Fra Expression in Mesoderm Redirects Muscle Precursors toward Slit-Expressing Midline Cells

(A) A wild-type stage 15 embryo stained with the FMM5 mAb to muscle myosin. The ventral midline is indicated by an arrow. At this stage, the ventral muscles are forming discrete groups and migrating toward their eventual insertion sites on the epidermis underneath the CNS. Anterior is left, dorsal is up.

(B) A stage 15 embryo expressing *robo-fra* under the control of the *24B-GAL4* pan-mesodermal driver stained with anti-Myc to visualize muscle and other mesodermal derivatives that are expressing the chimera. The development of muscles 7 and 6 (labeled), which are at a distance from the midline, appears to be normal. Anterior is left and dorsal is up.

(C) A stage 15 embryo expressing *robo-fra* stained with anti-Myc and anti-Slit. The ventral midline and Slit-expressing cells are indicated by an arrow with an asterisk. Slit staining can be seen as a faint blue stripe (Slit-expressing cells are out of the plane of focus). Muscle precursors can be seen inappropriately growing toward the Slit-expressing cells. These muscles have unusual morphology with many thin filopodia extending toward the midline. Anterior is left and dorsal is up.

(D) A view of the midline of the embryo shown in (B). We observe muscle precursors of unusual morphology extending toward the midline. The midline and Slit expression (blue stripe) are indicated by an arrow with an asterisk. Anterior is left and dorsal is up.

Such complex and dynamic behavior requires growth cones to be able to simultaneously respond to both attractants and repellents and to integrate these signals and respond to the relative balance of forces. Introducing a chimeric receptor into this finely tuned system leads to dramatic phenotypes. Adding a receptor that responds to Netrin as a repellent leads to a *comm*-like phenotype in which too few axons cross the midline. Adding a receptor that responds to Slit as an attractant leads to the opposite *robo*- or *slit*-like phenotypes, in which too many axons cross the midline or remain at the midline, respectively. These phenotypes are dose dependent, suggesting that by adding more chimeric receptor, we can tip the relative balance and thus selectively control the growth cone's response. This striking dosage sensitivity raises the possibility of using these phenotypes as the basis for genetic suppressor screens to identify signaling components that function downstream of attractive and repulsive guidance receptors.

Another finding of this study is that the signal transduction machinery for attraction and repulsion downstream of these receptors appears to be present in all neurons, and probably in all migrating muscle precursors as well. All neurons expressing Fra-Robo or Robo-Fra appear to behave the same, regardless of their environment. If they express Fra-Robo, they stay away from the midline; if they express Robo-Fra, they extend toward the midline. No other factor appears to intrinsically commit one growth cone or another to only one kind of response. The same is true for migrating muscle precursors. Normally, many of them express Robo (and Robo2; J. Simpson, T. Kidd, and C. S. G., unpublished results) and migrate away from the Slit-expressing midline (Kidd et al., 1999). However, given the opportunity (by transgenic expression of Robo-Fra), they clearly contain the full machinery for the opposite response. In all of our transgenic experiments, the growth cone or muscle response always correlated with the level of receptor.

Here we have shown that changing the receptor composition in vivo can alter the sign of a growth cone's response. Other recent studies have shown that changing the levels of cyclic nucleotides in vitro can lead to profound changes in the sign of a growth cone's response. Growth cones of embryonic *Xenopus laevis* spinal neurons grown in vitro exhibit chemoattraction toward Netrin-1 but show chemorepulsion in the presence of a competitive analog of cAMP or an inhibitor of protein kinase A (Ming et al., 1997). In contrast, Sema III, which normally is a repellent for growth cones of *Xenopus* spinal neurons in vitro, instead is converted to an attractant by activation of cGMP (Song et al., 1998).

These discoveries have important clinical implications because they suggest that cyclic nucleotides may be targets for therapeutics designed to block the inhibition of nerve regeneration. This potential is further supported by a recent study showing that increasing cAMP can block the ability of both myelin and myelin-associated glycoprotein (MAG) to inhibit axon regeneration in vitro (Cai et al., 1999). But these studies on cyclic nucleotides leave open the question of whether such dramatic changes in cyclic nucleotides normally occur in growth cones and whether they are used during development to determine the attractive versus repulsive response of growth cones.

The data presented here suggest that a key factor controlling attraction versus repulsion is the receptor's cytoplasmic domain. Different cytoplasmic domains or changes in cyclic nucleotides are not mutually exclusive explanations for how growth cone attraction versus repulsion is specified. For example, differences in the signaling output of the cytoplasmic domains of specific guidance receptors could lead to different effects on

cyclic nucleotide levels in the growth cone, which in turn could determine attraction versus repulsion. Alternatively, cyclic nucleotides could play an important modulatory function in helping to adjust the relative levels of responsiveness to different signals. The dramatic reversals of growth cone behavior observed in vitro may result from alterations in cAMP or cGMP levels beyond the normal physiological range occurring in growth cones.

The finding that the cytoplasmic sequence determines the response of a guidance receptor raises a number of interesting questions. Attraction might lead to a local change favoring actin polymerization over depolymerization, while repulsion might lead to the opposite change. But is guidance that simple? We now know the cytoplasmic sequences of five different families of repulsive guidance receptors: UNC-5s (Leung-Hagesteijn et al., 1992; Hamelin et al., 1993), Eph receptors (Cheng et al., 1995; Drescher et al., 1995), Neuropilins (Chen et al., 1997; He and Tessier-Lavigne, 1997; Kolodkin et al., 1997), Plexins (Comeau et al., 1998; Winberg et al., 1998b), and Robos (Kidd et al., 1998a). Interestingly, they appear to share little if any sequence similarity to one another in their cytoplasmic domains. It is possible, of course, that they bind different adapter proteins that converge on the same repulsive motility machinery. But it is equally likely that not all repulsion is the same and that different classes of repulsive receptors mediate different types of responses in the growth cone. It could be that what we lump together under the term "repulsion" are actually several molecularly distinct mechanisms that negatively influence local growth cone behavior. Just what these different cytoplasmic domains do, and how many different types of repulsion exist, awaits future investigation.

Experimental Procedures

Molecular Biology

Standard procedures were used to construct the Fra-Robo, FraΔC, Robo-Fra, and RoboΔC plasmids. For Fra-Robo, a 3.3 kb EcoRI/ClaI fragment containing the ectodomain of Fra, a 1.4 kb ClaI/SpeI fragment containing the transmembrane and cytoplasmic domain of Robo, and a 0.35 kb SpeI/NotI fragment containing six copies of a Myc epitope were amplified by PCR and cloned in pBluescript (pBS) to create pBS Fra-Robo-Myc. The junctions and large internal portions of the plasmid were sequenced. Fra-Robo-Myc was cloned into pUAST for transformation into flies. FraΔC-Myc was derived by internal deletion of Fra-Robo. Briefly, pBS Fra-Robo-Myc was cut to remove all but 230 nucleotides of Robo (the region encoding the transmembrane and first 67 amino acids of the cytoplasmic domain) and recircularized. The junctions were sequenced. For Robo-Fra, a Myc-tagged Robo cDNA was digested to remove all but 67 amino acids of the Robo cytoplasmic domain, creating RoboΔC-Myc. A 0.9 kb Fra fragment containing the cytoplasmic domain of Fra was generated by PCR, cloned into RoboΔC-Myc, and confirmed by sequencing. Robo-Fra-Myc and RoboΔC-Myc were cloned into pUAST for transformation into flies.

Fly Stocks and Transgenes

The following GAL4 stocks were used: *elav-GAL4, ftz$_{ng}$-GAL4, and 24B-GAL4*. At least four independent transformant lines were obtained for each construct. For the epistasis analysis of Fra-Robo, two recombinant third chromosomes were created: one that carried one copy of *fra-robo* and one copy of *elav-GAL4* (FR,E), and a second that carried two copies of *fra-robo* (FR2X). Animals that carry these chromosomes in *trans* are always commissureless (n > 100). This allows the Myc tag on *fra-robo* to be used as a molecular marker to identify the *fra-robo* gain-of-function animals. The following stocks and/or parental flies were created: (1) *netrin*/+; FR,E/TM2; (2) FR2X/FR2X; (3) *fra^{GA957}*/Cyo, *elav*β*-gal*; FR,E/TM2; and (4) *fra^{GA957}*/Cyo, *elav*β*-gal*; FR2X/FR2X. To test the dependence of the *fra-robo* gain-of-function phenotype on *netrin, netrin*/+; FR,E/TM2 females were crossed to FR2X/FR2X males. Progeny were stained with Myc antibodies to identify the *fra-robo* gain-of-function animals and BP102 to examine the axon scaffold. The genotype with respect to NP5 was either inferred from the characteristic *netrin* phenotype or directly examined by RNA in situ using a probe to *NetB*. One hundred and seven stage 15–16 embryos from the above cross were examined. Forty-one of those stained positive for Myc, indicating that they were *fra-robo* gain-of-function animals. Of these 41, one-fourth should be NP5 males. Thirteen of the forty-one displayed the NP5 phenotype, while the other twenty-eight were commissureless, consistent with the predicted one-fourth to three-fourth ratio. For *fra, fra^{GA957}*/Cyo, *elav*β*-gal*; FR,E/TM2 females were crossed to *fra^{GA957}*/Cyo, *elav*β*-gal*; FR2X/FR2X males, and progeny were stained with anti-β-gal antibodies to identify the *fra*-homozygous individuals and BP102 to examine the axon scaffold. Animals homozygous for *fra* were examined to see if any showed the commissureless phenotype associated with *fra-robo* gain of function. Nearly half of these animals showed the commissureless phenotype, while the other half showed the *fra* phenotype (34 commissureless, 39 *frazzled*). Direct examination by triple staining with BP102, Myc, and β-gal antibodies confirmed these observations.

To generate animals carrying *UAS commissureless* and the full complement of *fra-robo*, we created a stock that was homozygous for *UAS comm* on the X and homozygous for FR2X on the third: *UAS-comm/UAS-comm; FR2X/FR2X* females were crossed to males who were *FR,E/TM3actin*β*-gal*. Progeny were stained with anti-Sex-Lethal (to stain females), anti-β-gal (to stain TM3 flies), and BP102 to examine the axon scaffold. Progeny that stained only with BP102 were males that were *UAS-comm; FR,E/FR2X*. All of these animals showed a similar suppression of the *fra-robo* gain-of-function phenotype with some significant commissure formation in greater than 60% of segments (n = 29 animals).

Immunohistochemistry

Embryo-staining procedures were as previously described (Kidd et al. [1998a]).

Acknowledgments

We thank Ron Smith for superb technical assistance. We thank Julie Simpson, Theresa Ho, and Guochun Luo for preliminary work on the design of the Frazzled-Robo construct. We thank Tom Kidd, Kim Bland, and Julie Simpson at the University of California, Berkeley and Marc Tessier-Lavigne at the University of California, San Francisco for insightful discussions and exchange of data. We also thank Tom Kidd, Julie Simpson, and Kim Bland for valuable comments on the manuscript. G. J. B. is a Postdoctoral Fellow supported by the Cancer Research Fund of the Damon Runyon–Walter Winchell Foundation (DRG 1474). C. S. G. is an Investigator with the Howard Hughes Medical Institute. This work was supported by NIH grant NS18366 to C. S. G.

Received March 15, 1999; revised May 17, 1999.

References

Bagnard, D., Lohrum, M., Uziel, D., Püschel, A., and Bolz, J. (1998). Semaphorins act as attractive and repulsive guidance signals during the development of cortical projections. Development *125*, 5043–5053.

Brand, A.H., and Perrimon, N. (1993). Targeted gene expression as a means of altering cell fates and generating dominant phenotypes. Development *118*, 401–415.

Brose, K., Bland, K.S., Wang, K.H., Arnott, D., Henzel, W., Goodman, C.S., Tessier-Lavigne, M., and Kidd, T. (1999). Slit proteins bind Robo receptors and have an evolutionarily conserved role in repulsive axon guidance. Cell *96*, 795–806.

Cai, D., Shen, Y., Bellard, M., Tang, S., and Filbin, M.T. (1999). Prior exposure to neurotrophins blocks inhibition of axonal regeneration by MAG and myelin via a cAMP-dependent mechanism. Neuron *22*, 89–101.

Chan, S.S.-Y., Zheng, H., Su, M.-W., Wilk, R., Killeen, M.T., Hedgecock, E.M., and Culotti, J.G. (1996). UNC-40, a C. elegans homolog of DCC (Deleted in Colorectal Cancer), is required in motile cells responding to UNC-6 netrin cues. Cell *87*, 187–195.

Chen, H., Chédotal, A., He, Z., Goodman, C.S., and Tessier-Lavigne, M. (1997). Neuropilin-2, a novel member of the neuropilin family, is a high affinity receptor for the semaphorins Sema E and Sema IV but not Sema III. Neuron *19*, 547–559.

Cheng, H.J., Nakamoto, M., Bergemann, A.D., and Flanagan, J.G. (1995). Complementary gradients in expression and binding of ELF-1 and Mek4 in development of the topographic retinotectal projection map. Cell *82*, 371–381.

Colamarino, S.A., and Tessier-Lavigne, M. (1995). The axonal chemoattractant netrin-1 is also a chemorepellent for trochlear motor axons. Cell *81*, 621–629.

Comeau, M.R., Johnson, R., DuBose, R.F., Petersen, M., Gearing, P., VandenBos, T., Park, L., Farrah, T., Buller, R.M., et al. (1998). A poxvirus-encoded semaphorin induces cytokine production from monocytes and binds to a novel cellular semaphorin receptor, VESPR. Immunity *8*, 473–482.

Drescher, U., Kremoser, C., Handwerker, C., Loschinger, J., Noda, M., and Bonhoeffer, F. (1995). In vitro guidance of retinal ganglion cell axons by RAGS, a 25 kDa tectal protein related to ligands for Eph receptor tyrosine kinases. Cell *82*, 359–370.

Hamelin, M., Zhou, Y., Su, M.W., Scott, I.M., and Culotti, J.G. (1993). Expression of the UNC-5 guidance receptor in the touch neurons of C. elegans steers their axons dorsally. Nature *364*, 327–330.

Harris, R., Sabatelli, L.M., and Seeger, M.A. (1996). Guidance cues at the Drosophila CNS midline: identification and characterization of two Drosophila Netrin/UNC-6 homologs. Neuron *17*, 217–228.

He, Z., and Tessier-Lavigne, M. (1997). Neuropilin is a receptor for the axonal chemorepellent Semaphorin III. Cell *90*, 739–751.

Hedgecock, E.M., Culotti, J.G., and Hall, D.H. (1990). The unc-5, unc-6, and unc-40 genes guide circumferential migrations of pioneer axons and mesodermal cells on the epidermis in C. elegans. Neuron *4*, 61–85.

Hong, K., Hinck, L., Nishiyama, M., Poo, M.-M., Tessier-Lavigne, M., and Stein, E. (1999). A ligand-gated association between cytoplasmic domains of the UNC5 and DCC family receptors converts netrin-induced growth cone attraction to repulsion. Cell *97*, this issue, 927–941.

Keino-Masu, K., Masu, M., Hinck, L., Leonardo, E.D., Chan, S.S.-Y., Culotti, J.G., and Tessier-Lavigne, M. (1996). *Deleted in Colorectal Cancer (DCC)* encodes a Netrin receptor. Cell *87*, 175–185.

Kidd, T., Brose, K., Mitchell, K.J., Fetter, R.D., Tessier-Lavigne, M., Goodman, C.S., and Tear, G. (1998a). Roundabout controls axon crossing of the CNS midline and defines a novel subfamily of evolutionarily conserved guidance receptors. Cell *92*, 205–215.

Kidd, T., Russell, C., Goodman, C.S., and Tear, G. (1998b). Dosage-sensitive and complementary functions of Roundabout and Commissureless control axon crossing of the CNS midline. Neuron *20*, 25–33.

Kidd, T., Bland, K.S., and Goodman, C.S. (1999). Slit is the midline repellent for the Robo receptor in *Drosophila*. Cell *96*, 785–794.

Kolodkin, A.L., Matthes, D.J., and Goodman, C.S. (1993). The semaphorin genes encode a family of transmembrane and secreted growth cone guidance molecules. Cell *75*, 1389–1399.

Kolodkin, A.L., Levengood, D.V., Rowe, E.G., Tai, Y.T., Giger, R.J., and Ginty, D.D. (1997). Neuropilin is a semaphorin III receptor. Cell *90*, 753–762.

Kolodziej, P.A., Timpe, L.C., Mitchell, K.J., Fried, S.R., Goodman, C.S., Jan, L.Y., and Jan, Y.N. (1996). *frazzled* encodes a Drosophila member of the DCC immunoglobulin subfamily and is required for CNS and motor axon guidance. Cell *87*, 197–204.

Leung-Hagesteijn, C., Spence, A.M., Stern, B.D., Zhou, Y., Su, M.W., Hedgecock, E.M., and Culotti, J.G. (1992). UNC-5, a transmembrane protein with immunoglobulin and thrombospondin type 1 domains, guides cell and pioneer axon migrations in C. elegans. Cell *71*, 289–299.

Lewis, J.O., and Crews, S.T. (1994). Genetic analysis of the Drosophila *single-minded* gene reveals a central nervous system influence on muscle development. Mech. Dev. *48*, 81–91.

Li, H.-s., Chen, J.-h., Wu, W., Fagaly, T., Zhou, L., Yuan, W., Dupuis, S., Jiang, Z.-h., Nash, W., Gick, C., et al. (1999). Vertebrate Slit, a secreted ligand for the transmembrane protein Roundabout, is a repellent for olfactory bulb neurons. Cell *96*, 807–818.

Luo, Y., Raible, D., and Raper, J.A. (1993). Collapsin: a protein in brain that induces the collapse and paralysis of neuronal growth cones. Cell *75*, 217–227.

Ming, G.L., Song, H.J., Berninger, B., Holt, C.E., Tessier-Lavigne, M., and Poo, M.M. (1997). cAMP-dependent growth cone guidance by netrin-1. Neuron *19*, 1225–1235.

Mitchell, K.J., Doyle, J.L., Serafini, T., Kennedy, T.E., Tessier-Lavigne, M., Goodman, C.S., and Dickson, B.J. (1996). Genetic analysis of Netrin genes in Drosophila: Netrins guide CNS commissural axons and peripheral motor axons. Neuron *17*, 203–215.

Rothberg, J.M., Jacobs, J.R., Goodman, C.S., and Artavanis-Tsakonas, S. (1990). slit: an extracellular protein necessary for development of midline glia and commissural axon pathways contains both EGF and LRR domains. Genes Dev. *4*, 2169–2187.

Serafini, T., Kennedy, T.E., Galko, M.J., Mirzayan, C., Jessell, T.M., and Tessier-Lavigne, M. (1994). The netrins define a family of axon outgrowth-promoting proteins homologous to C. elegans UNC-6. Cell *78*, 409–424.

Song, H.J., Ming, G.L., He, Z., Lehmann, M., McKerracher, L., Tessier-Lavigne, M., and Poo, M.M. (1998). Conversion of neuronal growth cones responses from repulsion to attraction by cyclic nucleotides. Science *281*, 1515–1518.

Tessier-Lavigne, M., and Goodman, C.S. (1996). The molecular biology of axon guidance. Science *274*, 1123–1133.

Van Vactor, D., Sink, H., Fambrough, D., Tsoo, R., and Goodman, C.S. (1993). Genes that control neuromuscular specificity in Drosophila. Cell *73*, 1137–1153.

Wang, K.H., Brose, K., Arnott, D., Kidd, T., Goodman, C.S., Henzel, W., and Tessier-Lavigne, M. (1999). Biochemical purification of a mammalian Slit protein as a positive regulator of sensory axon elongation and branching. Cell *96*, 771–784.

Winberg, M.L., Mitchell, K.J., and Goodman, C.S. (1998a). Genetic analysis of the mechanisms controlling target selection: complementary and combinatorial functions of netrins, semaphorins, and IgCAMs. Cell *93*, 581–591.

Winberg, M.L., Noordermeer, J.N., Tamagnone, L., Comoglio, P.M., Spriggs, M.K., Tessier-Lavigne, M., and Goodman, C.S. (1998b). Plexin A is a neuronal semaphorin receptor that controls axon guidance. Cell *95*, 903–916.

Wong, J.T., Yu, W.T., and O'Connor, T.P. (1997). Transmembrane grasshopper Semaphorin I promotes axon outgrowth in vivo. Development *124*, 3597–3607.